

1 The Observed Evolution of Arctic Amplification over the Past 45

2 Years

3 Mark C. Serreze¹, Elizabeth Cassano^{1,2}, Alex Crawford³, John J. Cassano^{1,2}, and Chen Zhang^{1,2}

4 ¹Cooperative Institute for Research in Environmental Sciences, National Snow and Ice Data Center, University of
5 Colorado Boulder, CO, USA

6 ²Department of Atmospheric and Oceanic Sciences, University of Colorado Boulder, Boulder, CO, USA

7 ³Centre for Earth Observation Science, Department of Environment and Geography, University of Manitoba,
8 Winnipeg, MB, Canada

9

10 *Correspondence to:* Mark Serreze (mark.serreze@colorado.edu)

11 **Abstract.** To address research gaps in understanding Arctic Amplification, we use data from ERA5, [an observational](#)
12 [surface temperature dataset](#), and sea ice concentration to examine the seasonal, spatial and decadal evolution of
13 Arctic 2-meter and lower tropospheric temperatures and lower tropospheric (surface to 850 hPa) static stability over
14 the past 45 years. A Local Amplification Anomaly (LAA) metric is used to examine how spatial patterns of Arctic 2-
15 meter temperature anomalies compare to anomalies for the globe as a whole. Pointing to impacts of seasonally-delayed
16 albedo feedback, growing areas of end-of-summer (September) open water largely co-locate with the strongest
17 positive anomalies of 2-meter temperatures through autumn and winter and their growth through time; small summer
18 trends reflect the effects of a melting sea ice cover. Because of seasonal ice growth, the association between rising 2-
19 meter temperatures and sea ice weakens from autumn into winter, except in the ~~the~~ Barents Sea where there have been
20 prominent downward trends in winter ice extent. Imprints of variable atmospheric circulation are prominent in the
21 Arctic temperature evolution. Low-level (surface to 850 hPa) stability over the Arctic increases from autumn through
22 winter, consistent with the greater depth of surface-based atmospheric heating seen in autumn. However, trends
23 towards weaker static stability dominate the Arctic Ocean in autumn and winter, especially over areas of September
24 and wintertime ice loss. Sea ice thinning, leading to increased conductive heat fluxes through the ice, likely also
25 contributes to reduced stability.

26

27

28 Non-technical Summary

29 The outsized warming of the Arctic relative to the globe as a whole (Arctic Amplification) is largest in ~~in~~ autumn and
30 winter, consistent with large transfers of energy from growing areas of open water. Impacts of variable atmospheric
31 circulation are also prominent. AA is small in summer due to the melting sea ice cover. Warming penetrates higher
32 into the atmosphere in autumn compared to winter, but trends towards weaker stability could enable deeper heating
33 as AA further evolves.

34

35

36 **1 Introduction**

37 Arctic amplification (AA) refers to the observation that, over the last several decades, the rate of increase in surface
38 air temperature over the Arctic region has been larger than for the globe as a whole. [As reviewed by Esau et al. \(2023\),](#)
39 [AA is having impacts on Arctic terrestrial and marine ecosystems, permafrost conditions, ice sheets and glaciers as](#)
40 [well as human systems.](#) AA was predicted as a consequence of global warming even in the earliest generation of
41 climate models, and was envisioned as far back as the 19th century (Arrhenius, 1896). Various studies have placed the
42 ratio of Arctic to global warming from two to four, with differences relating to the definition of the Arctic region, data
43 used, the time period examined and the season examined (Yu et al., 2021a; Walsh, 2014; Richter Menge and
44 Druckenmiller, 2020; Jansen et al., 2020; AMAP, 2021; Rantanen et al., 2022). Using several observational data sets
45 and defining the Arctic as the region poleward of the Arctic Circle, Rantanen et al. (2022) find a factor of four warming
46 relative to the globe over the period 1979-2021 based on annual mean temperatures. From comparisons with climate
47 models, they conclude that this large ratio is either an extremely unlikely event, or that the models systematically
48 underestimate AA. Zhou et al. (2024) conclude that the externally forced amplification is three-fold, with natural
49 variability explaining the remainder. [The Polar Amplification Model Intercomparison Project \(PAMIP; Smith et al.,](#)
50 [2019\) further investigates the causes and consequences of polar amplification using a coordinated set of numerical](#)
51 [model experiments, providing valuable insights into the mechanisms driving AA.](#)

52 Growing spring and summer sea ice loss, leading to more seasonal heat gain in the ocean mixed layer and subsequent
53 upward heat release in autumn and winter - a seasonally-delayed expression of albedo feedback - is widely accepted
54 as a key driver of AA (Perovich et al., 2007; Steele et al., 2008; Serreze et al., 2009; Screen and Simmonds, 2010a,b;
55 Stammerjohn et al., 2012; Stroeve et al., 2014, Dai et al., 2019). However, based on observations and modeling studies,
56 AA is also recognized as involving a suite of connected contributions including changes in [atmospheric circulation](#)
57 [and poleward energy transport \(Graversen and Burt et al., 2016; Woods and Caballero, 2016; Henderson et al., 2021;](#)
58 [Previdi et al., 2021, Zhang et al., 2025\)](#), Planck feedback (Pithan and Mauritsen, 2014), positive lapse rate feedback
59 (Pithan and Mauritsen, 2014; Stuecker et al., 2018; Previdi et al., 2021), changes in ocean heat transport (Beer et al.,
60 2020), changes in autumn cloud cover (Kay and Gettelman, 2009; Wu and Lee, 2012) and even reduced air pollution
61 in Europe (Navarro et al., 2016; Krishnan et al., 2020). [Taylor et al. \(2022\) provide an insightful history of AA science.](#)

62 However, much remains to be understood about AA, [notably, the spatial aspects of its observed evolution, seasonal](#)
63 [shifts in its expression and evolution, and the its regional expression vertical structure of AA in the context of changing](#)
64 [static stability. s, and overall evolution.](#) Here, using data from the ERA5 reanalysis, [surface temperature observations,](#)
65 and satellite-derived sea ice concentration, we focus on understanding the decadal evolution and seasonal/spatial
66 expressions of Arctic temperature anomalies. [The local characteristics of AA are important, as regional variations can](#)
67 [produce different remote influences, including midlatitude climate extremes \(Zhou et al., 2023\).](#) We show how: 1) the
68 pronounced autumn contribution to AA, through which internal energy gained by the upper ocean in spring and
69 summer in growing open water areas is subsequently released back to the atmosphere, decays into winter as sea ice
70 forms (the exception being in the Barents Sea sector, which has seen pronounced winter ice losses); 2) The decadal
71 evolution of AA is modulated by variable spatial expressions of atmospheric circulation; 3) the deeper vertical extent

72 of pronounced temperature anomalies in autumn than winter is consistent with the seasonal increase in static stability
73 from autumn to winter; and 4) reductions in static stability in autumn point toward increasingly deep penetration of
74 surface warming into the troposphere with continued sea ice loss, and potentially greater impacts of AA on altering
75 weather patterns in lower latitudes (Ding et al., 2024).

76 **2 Data Sources**

77 Data from the European Centre for Medium-range Weather Forecasts (ECMWF) reanalysis (ERA5; Hersbach et al.,
78 2020) are used for analysis. Monthly temperature (2 m and the significant levels from 1000 to 500 hPa) and surface
79 and latent heat fluxes~~sea level pressure~~ were used on the $0.25^\circ \times 0.25^\circ$ horizontal grid from 1979-2024. While ERA5
80 data are available since 1950, fields since 1979, the advent of the modern satellite database for assimilation, are more
81 reliable. ERA5 is chosen because, in various comparisons of (near-) surface parameters throughout the Arctic, ERA5
82 performs similarly to or better than other global and regional reanalysis products (Graham et al., 2019; Barrett et al.,
83 2020; Renfrew et al., 2021; Crawford et al., 2022). Reliance is placed on trends and anomalies. Anomalies are
84 referenced to the 30-year period 1981-2010, but comparisons are made with different averaging periods. To assess
85 relationships with sea ice conditions, we use the satellite passive microwave records from the National Snow and Ice
86 Data Center. The satellite passive microwave record provides estimates of concentration and extent from October
87 1978 through the present at 25-km resolution on a polar stereographic grid (~~the EASE2 grid~~) by combining data from
88 the Nimbus-7 Scanning Multichannel Microwave Radiometer (SMMR, 1979–1987), the Defense Meteorological
89 Satellite Program (DMSP) Special Sensor Microwave/Imager (SSM/I, 1987–2007) and the Special Sensor Microwave
90 Imager/Sounder (SSMIS, 2007-onwards) (Fetterer et al., 2002).

91

92 Our results must be viewed within the context of known problems in ERA5, one being a warm bias in 2-meter air
93 temperature over the Arctic (Yu et al., 2021b; Tian et al., 2024). Compared to an extensive set of matching drifting
94 observations, Yu et al. (2021b) found ERA5 to have a mean bias of $2.34 \pm 3.22^\circ\text{C}$ in 2-meter air temperature, largest
95 in April and smallest in September. Interestingly, surface (skin) temperature biases were found to be negative (-4.11
96 $\pm 3.92^\circ\text{C}$ overall, largest in December and smaller in the warmer months), although the magnitudes might be
97 overestimated by the location of the surface temperature sensors on the buoys, which may have been affected by snow
98 cover. While we are largely dealing in this paper with anomalies, rather than absolute values, our comparisons between
99 Arctic and global anomalies may be influenced by the fact that biases at the global scale are different. Wang et al.
100 (2019) found that compared to the earlier ERA-I effort, ERA5 has a larger warm bias at very low temperatures (< -25°C)
101 but a smaller bias at higher temperatures. ERA5 has higher total precipitation and snowfall over Arctic sea ice.
102 The snowpack in ERA5 results in less heat loss to the atmosphere and hence -thinner ice at the end of the growth
103 season, despite the warm bias.

104

105 To further address biases in ERA5, analysis was also performed using the Berkeley Earth Surface Temperatures
106 (BEST) gridded surface temperature data (Rohde and Hausfather, 2020; Available for download from:
107 <https://berkeleyearth.org/data/>). This dataset extends back to 1850, combining both 2m temperatures over land as well

108 as sea surface temperatures to create a global, gridded observational dataset to which reanalysis data can be compared.

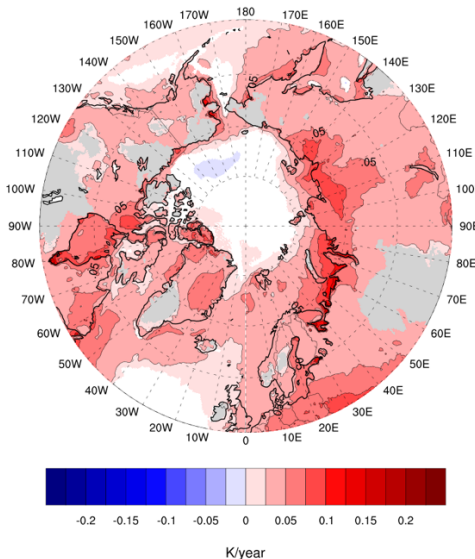
109

110 **3 Results**

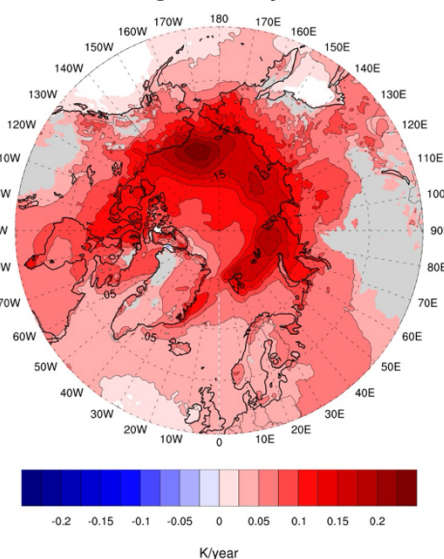
111 **3.1 Seasonality of 2-Meter Temperature Trends**

112 A key, but in our view, under-appreciated aspect of AA is its strong seasonality - under-appreciated not that it exists
113 but in the sense that processes at work during summer over the Arctic Ocean, when AA is small, set the stage for
114 understanding the strong imprints of AA during autumn and winter. Rantanen et al. (2022) foundfind that the AA
115 factor as assessed for the region poleward of the Arctic circle ranges from less than 2two in July to over 5five in
116 November. Climate models examined in that study largely capture this seasonality but with smaller amplification
117 factors. Figure 1 shows spatial patterns of surface air temperature trends by season based on ERA5. In this study, the
118 Arctic is defined as areas poleward of 60°N, but mapsThese plots extend down to 50°N to enable comparisons between
119 changes in the Arctic and the higher middle latitudes. The same analysis but performed with the BEST data are shown
120 in Supplemental Figure 1. The description of the results from these figures apply to both datasets except where
121 explicitly stated.

(a) JJA change in T2M /year 1980-2024

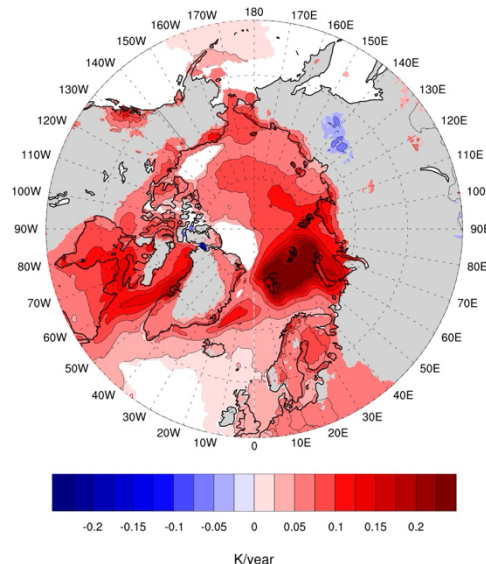


(b) SON change in T2M /year 1980-2024

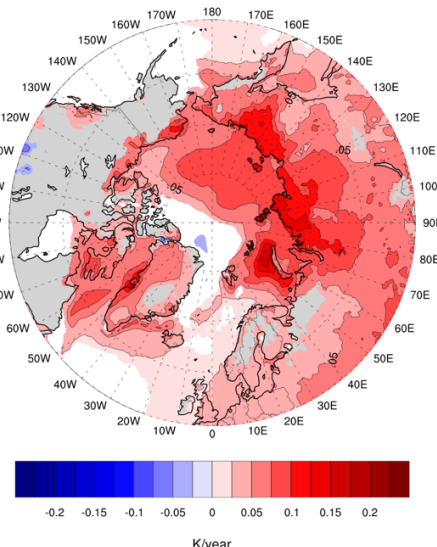


122

(c) DJF change in T2M /year 1980-2024



(d) MAM change in T2M /year 1980-2024



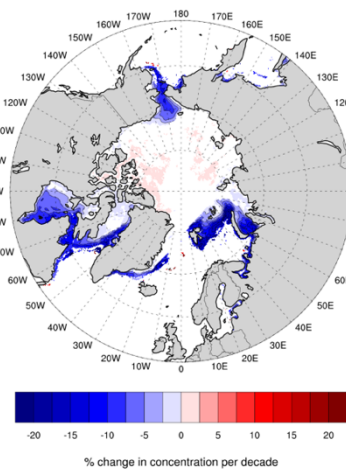
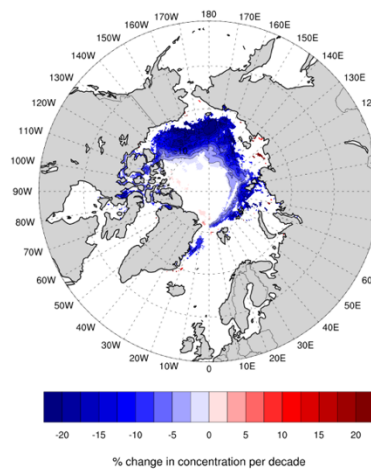
123

124

125 Figure 1: Linear trends in ERA5 2-meter temperatures (T2M) -by season from 1980 to 2024, in degrees per year for (aA)
126 June, July, August (JJA), (bB) September, October, November (SON), (cC) December, January, February (DJF) and
127 (dD) March, April, May (MAM). Only trends significant at $p < 0.05$ are shaded based on an ordinary least squares
128 regression test. Shading is used for trends significant at $p < 0.05$.

129

(a) Sep percent change in seaice concentration/decade 1980-2024 (b) Dec percent change in seaice concentration/decade 1980-2024



130

131 Figure 2: Linear trends in sea ice concentration %/per decade 1980 through 2024 for September (aleft) and December
132 (bright). Only trends significant at $p < 0.05$ are shaded based on an ordinary least squares regression test.

133

134 The sharply smaller trends in summer compared to autumn and winter across Arctic latitudes clearly stands out. In
135 interpreting these patterns, we focus on broad, contiguous regions rather than isolated grid points that may be affected

136 by spatial autocorrelation. Summer trends are nevertheless largely positive and statistically significant across most of
137 the Arctic and subarctic lands. Trends in ERA5 are very small and not statistically significant across the central Arctic
138 Ocean, while in the BEST data, the trends over the Arctic Ocean are significant, albeit still small (Figure S1a). Since
139 the skin temperature of a melting sea ice cover is pegged to the melting point, it follows that surface air temperature
140 trends must be small in this area. Over land, earlier loss of the snow cover (Mudryk et al., 2023) likely contributes to
141 the rise in surface air temperatures seen there. Trends along the Russian and Alaska coastline are also positive. Melt
142 onset typically starts in June in the southern margins of the ice cover and progresses poleward (Markus et al., 2009).
143 Positive trends along the coastal seas are consistent with satellite observations of both a progressively earlier onset of
144 melt (Stroeve et al., 2014; Stroeve and Notz, 2018). They are also consistent with progressively earlier exposure of
145 dark open water areas, their expanding coverage through time, and associated increased internal energy in the ocean
146 mixed layer (Perovich et al., 2007; Serreze et al., 2009; Perovich and Polashenski, 2012; Stammerjohn et al., 2012;
147 Dai et al., 2019; Li et al., 2021¹²; Bianco et al., 2024). However, the large specific heat of water and the depth of
148 heating (10-30 m) will limit the rise in surface air temperature. Note also the positive trends over the northern North
149 Atlantic, which is ice-free over the entire year. Somewhat larger trends are found over part of the Kara and Barents
150 Seas.

151 The largest temperature trends for autumn, locally exceeding 0.2°C per year, lie primarily on the Eurasian side of the
152 Arctic Ocean and north of Alaska. A comparison to the spatial pattern of September (end of summer) sea ice
153 concentration (Figure 2), provides an understanding: the trends are largest in those areas with the sharpest downward
154 trends in ice concentration, most notably in the Chukchi and East Siberian Seas and hence where there will be strong
155 upward surface heat fluxes as the ocean loses the internal energy it gained in summer. Our¹³The interpretation, building
156 from the above discussion and from earlier studies (e.g., Stammerjohn et al., 2012; Stroeve et al., 2016; Lebrun et al.,
157 2019), is that through the years, ice begins to retreat earlier and earlier in spring and summer, largely from the shores
158 of Alaska and the Russian coast, exposing areas of dark open water, which absorbs solar energy. This means more
159 energy gain in the ocean mixed layer, and over an increasingly large area, with time. As solar radiation declines in
160 autumn, this energy is released upwards to the atmosphere, seen as positive temperature anomalies that grow in
161 magnitude and spatial coverage with time. Before sea ice forms, all of the internal energy gained in summer must be
162 depleted.

163 The pattern of winter temperature trends is quite different. The positive trends along the Eurasian coastline and in the
164 Chukchi and Barents Seas are greatly reduced, and the largest trends, exceeding 0.2°C per year, are now located in
165 the Barents Sea. The reason for this is clear: By December, the areas of open water along the coast have re-frozen,
166 reducing energy transfer between the ocean and atmosphere¹⁴atmospheric heat fluxes limiting the ocean to atmosphere
167 heat fluxes. The Barents Sea is, in turn, one of the few areas with a substantial downward trend in winter sea ice extent
168 (Figure 2b¹⁵right panel). Still, positive 2-meter temperature trends in both autumn and winter encompass much of the
169 Arctic Ocean away from areas of ice loss. One likely driver of this is progressive thinning of the ice cover (Landy et
170 al., 2022; Sumata et al., 2023), allowing for an increase in conductive fluxes through the ice (Liu and Zhang, 2025).
Autumn and winter trends in sensible and latent heat fluxes from ERA5 show an increase over the time period of study

172 [of these fluxes from the surface to the atmosphere \(Supplemental Figure S2\)](#). Another driver is likely polar temperature
173 advection from the areas of sea ice loss (Timmermans et al., 2018), as evidenced by the tongue of fairly large positive
174 trends extending from the Barents Sea into the Arctic Ocean. Also of interest is that trends ~~over~~ much of the land
175 area are very small, even negative, especially over Eurasia.

176 By spring, the magnitude of temperature trends [in both the ERA5 and BEST data](#) over the Barents Sea has dropped
177 relative to winter, but is still prominent. Through spring, downward trends in sea ice concentration (not shown) persist,
178 but, compared to winter, air-sea temperature differences are smaller, hence ocean to atmosphere surface heat fluxes
179 are smaller. Substantial positive trends are found along the Eurasian coast, again suggestive of the role of atmospheric
180 heat advection. Trends over much of high-latitude North America are small.

181 To summarize, it is apparent that an assessment of Arctic Amplification based on comparing the Arctic trend with the
182 trend for the globe as a whole must recognize the highly pronounced seasonal and spatial heterogeneity of Arctic
183 trends. Summer 2-m temperature trends are mostly small, but the smallness over the Arctic Ocean is due to the melting
184 of ice. The much larger autumn trends reflect energy transfer from the ocean to the atmosphere via upward surface
185 heat fluxes from increasing extensive areas of open water. By winter, open water areas along the Eurasian coast and
186 the Chukchi Sea have re-frozen and the locus of maximum temperature trends is shifted to the Barents Seas, consistent
187 with the downward trends in sea ice concentration there. Spring trends are weaker than winter trends, but are still large
188 in the Barents Sea sector. However, for autumn, winter and spring, there are also features in the spatial patterns of
189 trends that point to advection and other processes, and winter trends in particular are small over much of the land area.

190 **3.2 Local Amplification Anomaly Approach**

191 To gain further insight into trends, we now look at the evolution of AA by decade, 1980-1989, 1990-1999, 2000-2009,
192 and 2010-2019, as well as the last five years of the record, 2020-2024, making use of what we term a Local
193 Amplification Anomaly (LAA) approach.

194 For each of these periods, we calculated the average 2-meter temperature at each ERA5 [and BEST](#) grid point across
195 the globe, then calculated the anomalies at each grid point relative to the 1981-2010 climatology. Taking the (spatially
196 weighted) average of all grid point anomalies yields the global temperature anomaly for each period. Then, at each
197 grid point we subtracted this global temperature anomaly from the anomaly at that point. We then compiled maps of
198 the anomalies for the region poleward of 50°N [\(including the Arctic \(north of 60°N\) and the sub-Arctic \(50-60°N\)\)](#).
199 Examining these LAAs gives us a sense of the spatial structure of Arctic temperature anomalies in terms of how they
200 contribute to the overall AA evolution. In Table 1 we also provide, for each decade and season, the average of the
201 anomalies relative to the global average poleward of 60°N and the average global anomaly. Results that follow will
202 of course reflect the chosen 1981-2010 referencing period.

	Global Anomaly (K)		Arctic Anomaly (K)		Difference (Arctic – Global; K)	
	BEST	ERA5	BEST	ERA5	BEST	ERA5
Autumn						
1980-1989	-0.22	-0.22	-0.76	-0.74	-0.54	-0.52
1990-1999	-0.05	-0.06	-0.35	-0.45	-0.30	-0.39
2000-2019	0.22	0.22	0.83	0.91	0.61	0.69
2010-2019	0.42	0.45	1.51	1.68	1.09	1.23
2020-2024	0.69	0.78	2.08	2.42	1.39	1.64
Winter						
1980-1989	-0.10	-0.16	-0.47	-0.24	-0.37	-0.08
1990-1999	-0.02	-0.03	-0.56	-0.53	-0.54	-0.50
2000-2009	0.15	0.16	0.73	0.71	0.58	0.55
2010-2019	0.35	0.38	1.66	1.66	1.31	1.28
2020-2024	0.54	0.62	1.35	1.38	0.81	0.76
Spring						
1980-1989	-0.20	-0.14	-0.83	-0.68	-0.63	-0.54
1990-1999	-0.01	-0.04	0.23	0.13	0.24	0.17
2000-2009	0.16	0.14	0.36	0.36	0.20	0.22
2010-2019	0.40	0.40	1.40	1.37	1.00	0.97
2020-2024	0.58	0.60	1.37	1.16	0.79	0.56
Summer						
1980-1989	-0.18	-0.15	-0.34	-0.29	0.16	-0.14
1990-1999	-0.001	-0.01	-0.09	-0.09	0.091	-0.08
2000-2009	0.14	0.13	0.33	0.28	0.19	0.15
2010-2019	0.34	0.35	0.64	0.70	0.30	0.35
2020-2024	0.61	0.63	0.86	1.04	0.25	0.41

204 **Table 1: Average temperature anomalies (K $^{\circ}$ C; with respect to 1981-2010) for the Arctic (north of 60 $^{\circ}$ N), the globe, and**
 205 **their difference for the BEST and ERA5 data.**

206 Results for autumn are examined first ([Figure 3 \(ERA5\)](#) and [Supplemental Figure 3 \(BEST data\)](#)). The description of
 207 the results apply to both datasets unless indicated otherwise. For the first two decades, 1980-1989 and 1990-1999,
 208 both the average global anomaly and the average Arctic anomaly are small and negative, with the Arctic anomalies
 209 actually more negative than the global value. [Since 1980-1989 is \(primarily\) the first decade of the 1981-2010 baseline](#)
 210 [period, greater negative anomalies for the Arctic than the globe still indicate amplified warming in the Arctic.](#)
 211 [Likewise, as](#) the middle of the baseline period, [1990-1999 experiences \(1981-2010\), the smallest anomalies are](#)
 212 [expressed in 1990-1999.](#) This pattern reverses starting in the 2000-2009 decade. -What this is capturing is that early
 213 in the record, the poleward gradient in 2-meter temperatures was stronger than it is today; as AA evolves, the gradient
 214 obviously weakens.

215 For the first decade, 1980-1989, LAAs are generally small across the Arctic, with a mix of positive and negative
 216 values, but with the negative anomalies obviously dominating (not shown). The exception is in the Chukchi Sea, where
 217 strong negative LAA values of up to 3 $^{\circ}$ C are found. Based on data from 1979-1996, Parkinson et al. (1999) showed
 218 downward trends in ice concentration in the Chukchi Sea of around 4% per decade. However, as the area had more

219 sea ice in the 1980-1989 decade relative to the 1981-2010 climatology, it shows up as negative LAA values [in Figure](#)
220 [3](#).

221 As noted, in the 1990-1999 decade, both the Arctic average and the global average anomaly are at their minimum,
222 since this decade is in the middle of the 1981-2010 baseline (Table 1). [However, t](#)~~T~~he difference between the 1990-
223 1999 and the subsequent 2000-2009 decade is striking. Both the Arctic and global average anomalies are ~~now~~ positive
224 ([Table 1, Figures 3 and S3](#)). Positive LAA values encompass most of the Arctic. The largest positive LAA values lie
225 in the Chukchi and East Siberian Seas, reflecting the continuing development through this decade of extensive open
226 waters in September ([Figures 3 and S3](#)). Note that the first clear indication of the emergence of AA related to sea ice
227 loss was based on data extending through the end of the 2000-2009 decade (Serreze et al., 2009; Screen et al., 2010a,b).
228 Wang et al. (2017) similarly found the emergence of amplified temperature anomalies over the Arctic (60-90°N)
229 compared to the northern mid-latitudes (30-60°N) in this decade. By the 2010-2019 decade, autumn LAA values of
230 [3-5°C in the ERA5 data \(2-4°C in the BEST data\)](#) are now prominent along the entire Eurasian coast and in the
231 Chukchi Sea; consistent with the continued increase in open water areas in September. Much smaller AA values
232 encompass most of the rest of the Arctic.

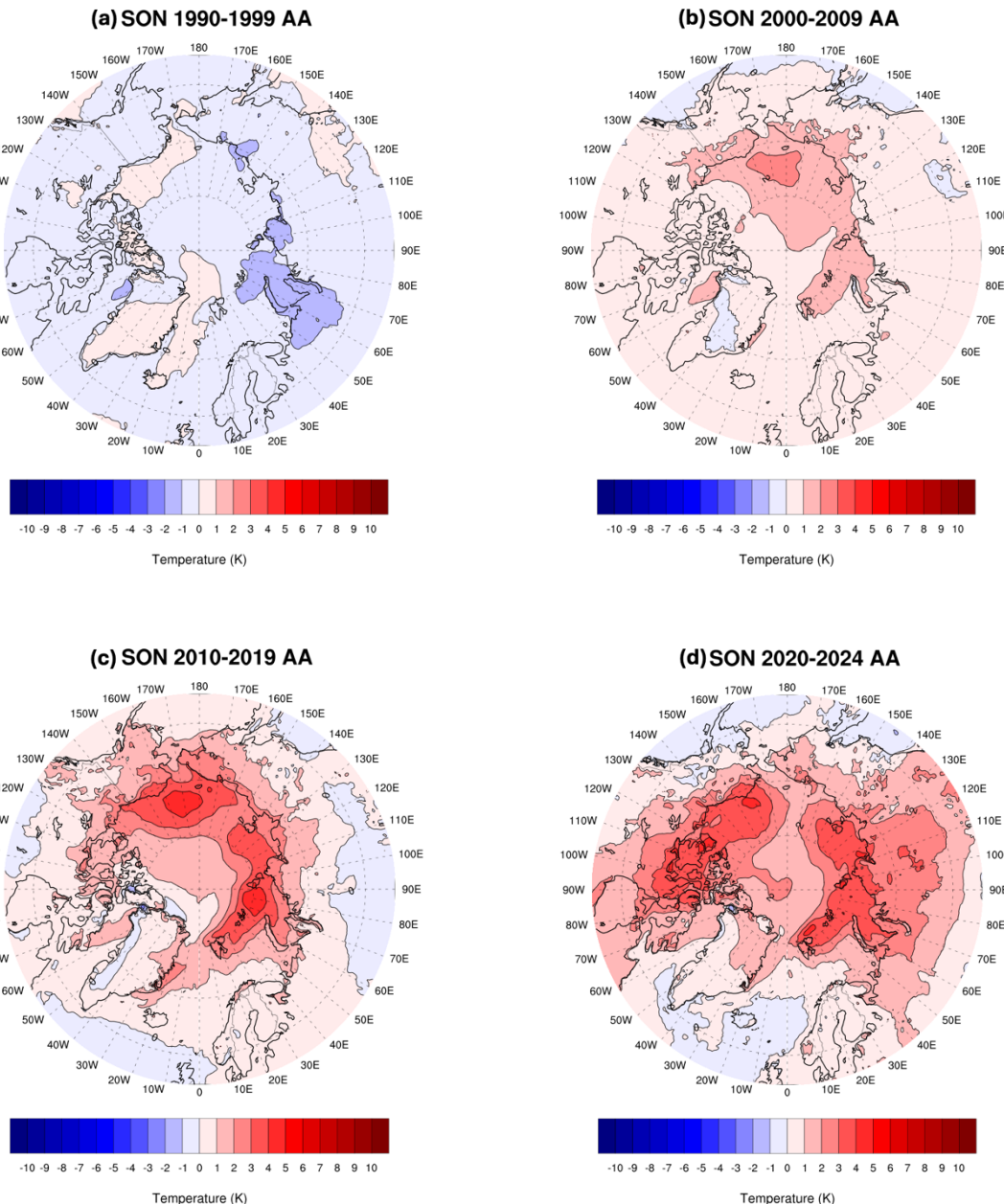
233 The most recent period, 2020-2024, sees a shift. While strongly positive anomalies relative to global average
234 anomalies - that is, positive LAA values ~~–~~ remain over much of the Eurasian coastal sea, LAA anomalies over the
235 Chukchi Sea are now smaller, and larger values have appeared in the Beaufort Sea and the Canadian Arctic
236 Archipelago. In explanation, when Arctic sea ice extent began to decline, it was initially most prominent in the
237 Chukchi Sea region, so LAA values there are especially large, as seen in the 2009-2009 and 2010-2019 plots. With
238 the rise in the global temperature anomalies, these LAA values become more subdued.

239 The winter evolution is quite different. ~~-~~The Arctic-averaged anomaly and the global anomaly for the 1980-1989 are
240 small and quite alike – AA had not yet emerged (Table 1). In terms of the LAA structure (not shown), positive values
241 of typically 1-2°C over much of Eurasia, Alaska and Canada contrast with negative values of similar size elsewhere,
242 the exception being negative values of 2-3°C in the Barents Sea sector. ~~-~~The story is similar for the 1990-1999 decade
243 - AA had yet to clearly emerge (Table 1), and, indeed, the Arctic average anomaly was about half a degree colder than
244 the global average anomaly. The LAA structure leading to this interesting finding is characterized by partly offsetting
245 positive and negative values ([Figure 4 \(ERA5\) and Supplemental Figure 4 \(BEST data\)\)](#). [As was the case for the](#)
246 [discussion of the autumn AA, the description of the results applies to both datasets unless indicated otherwise.\)](#) Of
247 interest in this regard is that North Atlantic Oscillation (or Arctic Oscillation) shifted from a negative to a strongly
248 positive index phase between the 1970s and late 1990s. Numerous studies examined the strong temperature trends
249 associated with this shift, notably warming over northern Eurasia, with cooling over northeastern Canada and
250 Greenland (e.g., Hurrell, 1995; 1996; Thompson and Wallace, 1998). There was vibrant debate over whether the shift
251 might be in part a result of greenhouse gas forcing and an emerging signal of expected Arctic Amplification (see the
252 review in Serreze et al., 2000).

253

254

255



256

257

258 **Figure 3. Autumn (September, October, November (SON)) ERA5 2-m temperature anomalies in °C relative to 1981-2010**
259 for **(a) 1990-1999, (b) 2000-2009, (c) 2010-2019 and (d) 2020-2024** minus the global average temperature anomaly for each
260 period.

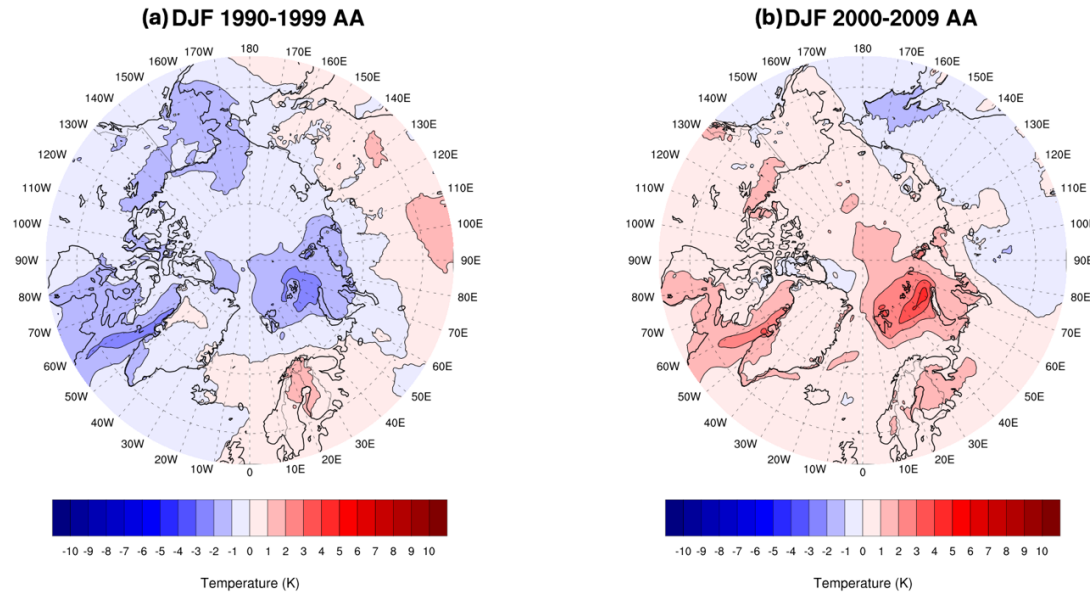
261 While there is some indication of a structure in LAA values for the 1990-1999 decade reminiscent of the rising phase
262 of the NAO over this time (note that the index value subsequently ~~decreased~~~~regressed~~), looking back to Table 1, the
263 behavior of the NAO clearly did not “boost” any emerging AA signal.

264 Turning to the decade 2000-2009, positive LAA values have become more dominant, and fairly large positive values
265 have appeared over the Barents Sea sector, replacing the negative values of the previous decade. While by this decade,
266 AA had clearly emerged (Table 1), note that the positive LAA values over northern Eurasia in 1990-1999 are replaced
267 by negative values, indicative of a circulation shift, notably, regression of the NAO from its previous high index
268 values.

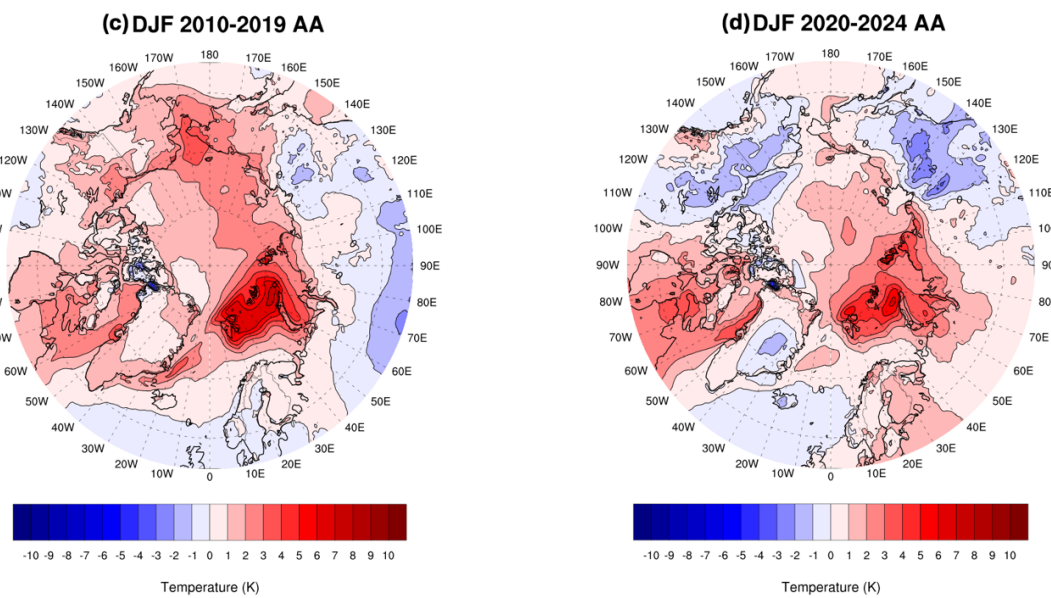
269 The 2010-2019 period is characterized by the emergence of large positive LAA values over the Barents Sea sector
270 which have intensified~~grown~~ since the 2000-2009 decade, pointing to the effects of growing open water areas in this
271 sector. Positive LAA values also cover almost all Arctic latitudes. The Barents Sea feature remains prominent in the
272 past five years of the record (2020-2024). Note, however, the negative anomalies over Alaska and eastern Eurasia. As
273 a result, the difference between the Arctic average temperature anomaly and the global average anomaly is actually
274 smaller than in the 2010-2019 period, that is, pan-Arctic AA is somewhat smaller. Note also by comparison with the
275 decade 2010-2019, LAA values along most of the Eurasia coast are less pronounced. This is understood in that, by
276 December, all areas along the Eurasian coast and north of the Chukchi and East Siberian seas have refrozen.

277 The observation that the last three time periods have negative LAA values over Eurasia is of interest through its
278 apparent link with Warm Arctic-Cold Eurasia (WACE) phenomenon -while AA has become increasingly prominent,
279 this has been attended by recent surface cooling over Eurasia, most evident in winter with considerable decadal
280 variability. (e.g., Gong et al., 2017; Li et al. 2021). The WACE phenomenon has garnered considerable attention over
281 the past decades and a suite of driving factors have been offered. An Urals blocking pattern has been identified as
282 playing a strong role, and recent work has shown that decadal variability in the WACE phenomenon is mediated by
283 phases of the Pacific Oscillation and the Atlantic Multidecadal Oscillation (e.g., Luo et al., 2022).

284 Turning back to the Barents Sea sector, it is notable that this is one of the few areas of the Arctic (along with eastern
285 Hudson Bay/Hudson Strait and Bering Strait, see Figure 2) with substantial downward trends in winter sea ice
286 concentration. Various studies have attributed the loss of winter ice in the Barents Sea and associated temperature
287 anomalies and trends to processes involving atmospheric circulation, facilitating~~promoting~~ intrusions of warm moist
288 air into the region with wind patterns promoting stronger transport of warm Atlantic waters into the region (Woods
289 and Caballero, 2016; Lien et al., 2017; Siew et al., 2024). Warm and moist air advection raises temperatures, inhibits
290 autumn and winter sea ice growth (Woods and Caballero, 2016; Crawford et al., 2025; Lee et al., 2017), and enhances
291 spring and summer ice melt (Kapsch et al., 2013; Park et al., 2015). Intrusions of Atlantic-derived waters, which
292 appear to be in part wind driven, also discourage winter ice growth. Beer et al. (2020) identified edy an oceanic
293 mechanism that increases the vertical heat flux in the upper Arctic Ocean under global warming that causes increased
294 ocean heat transport into the Arctic, which appears as a substantial contributor to Arctic Amplification.



295



296

297

298 **Figure 4: Winter (December, January, February, DJF) surface temperature anomalies in °C relative to 1981-2010 for (a)**
 299 **1990-1999, (b) 2000-2009, (c) 2010-2019 and (d) 2020-2024 minus the global average temperature anomaly for each**
 300 **period.**

301 While our primary focus is on the evolution of AA and LAAs in autumn and winter, it is warranted to briefly discuss
 302 spring and summer (not shown). The spring pattern of LAAs for the 1980-1989 decade is characterized by small and
 303 mostly negative values across the Arctic, transitioning to a mix between small positive and negative values for the

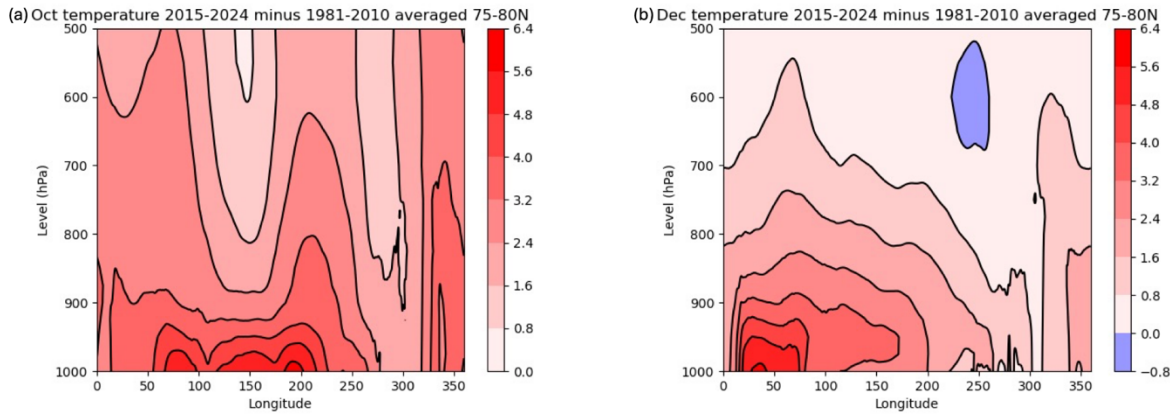
304 1990-1999 decade, as well as for the 2000-2010 decade. The largest difference between the Arctic average and global
305 average anomaly was for the 2010-2019 decade. This is consistent with the much smaller AA in this season compared
306 to autumn and winter. Only for the last five years of the record, 2020-2024 do prominent positive LAA values of over
307 3°C appear over Eurasia, but these are partly balanced by negative LAAs elsewhere and may represent short-term
308 internal variability. This is consistent with the much smaller AA in this season compared to autumn and winter. The
309 key feature of summer is that while as the decades pass, modest positive values of LAA appear over land, values
310 remain close to zero over the Arctic Ocean, reflecting the effects of the melting sea ice surface. The last five years
311 also show positive LAA values of up to 3°C along the shores of Eurasia, likely due to the open coastal waters in these
312 areas.

313 The results just discussed are with reference to 1981-2010 averages. Use of an earlier climatology (e.g., 1951-1980)
314 naturally yields stronger positive anomalies and weaker negative LAA values in the later part of the temperature
315 records, while a more recent climatology (e.g., 1991-2020, the current NOAA standard) has the opposite effect. The
316 1981-2010 reference applied in used on this paper, used by NOAA until the end of 2020, is an appropriate middle
317 ground, and is the reference period used for sea ice analyses by the National Snow and Ice Data Center ([Scott, 2022](#)).

318 3.3 Vertical Structure

319 An assessment of the vertical structure of warming helps to both highlight the effects of sea ice and shed light on other
320 processes known to be involved in Arctic Amplification, notably, static stability. To this end, we look at longitudinal
321 cross sections of temperature anomalies for the most recent 10 years of the record, averaged between the
322 latitudes longitudes 75-80°N, which corresponds to the latitude band with pronounced anomalies in surface air
323 temperature across both SON and DJF. We look first at October, then turn attention to December (Figure 5). October
324 is when there will be particularly large heat fluxes from the ocean to atmosphere, while in December, most of these
325 areas (apart from the Barents Sea) have re-frozen. This choice of months is intended to capture that contrast.

326 The strongly positive anomalies located from 60-120°E and between 180°E to 120°W (these being stronger) are clearly
327 surface-based, which makes sense as they are due to strong upward surface heat fluxes. The more prominent feature
328 between 180°E and 120°W (centered along the East Siberian and Chukchi Seas) is notable in that anomalies of 3°C
329 extend up to 700hPa. The December cross section shows maximum surface-based temperature anomalies focused
330 between about 20-70°E (centered near the Barents Sea), but positive anomalies do not extend as far in the vertical
331 compared to October. Although these anomalies are less vertically extensive, the stronger near-surface temperature
332 difference between the surface and the air above in December could potentially enhance surface fluxes.



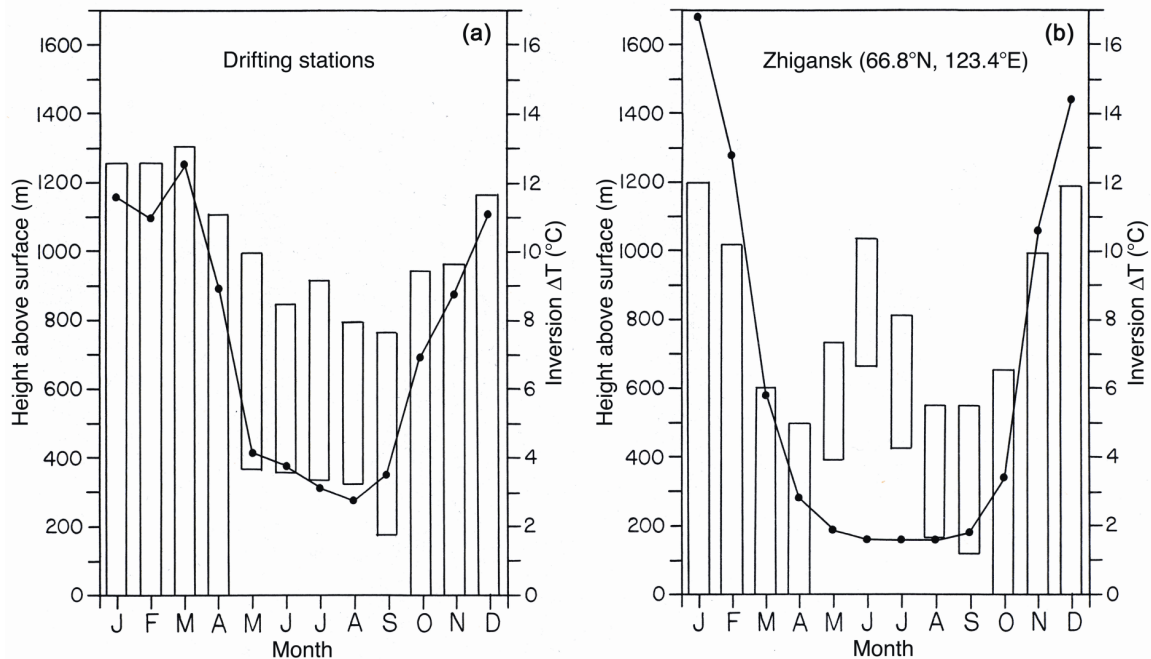
333

334 **Figure 5: Vertical cross sections by longitude across latitudes 75°N to 80°N for October (left) and December (right) of**
 335 **temperature anomalies for 2015-2024 minus 1981-2010.**

336 **3.4 Static Stability**

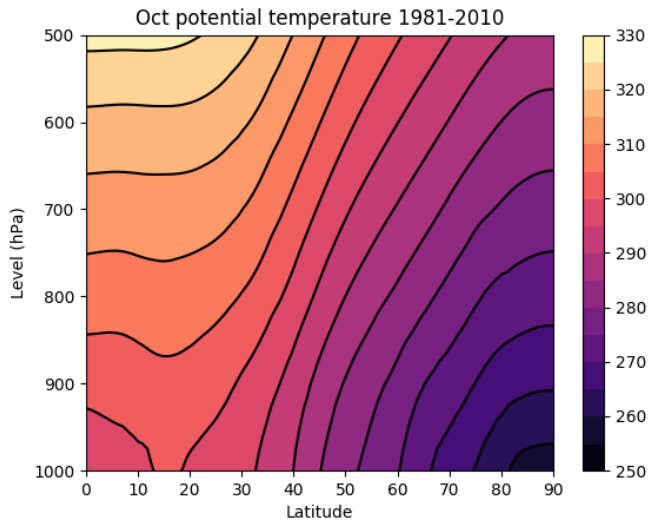
337 While the magnitude of the surface temperature anomaly will bear on how high in the vertical positive anomalies will
 338 persist, the vertical stability will play a role. The strong stability of the lower Arctic troposphere has long been
 339 recognized (Wexler, 1936; Bradley et al., 1992; Kahl et al., 1992; Serreze et al., 1992) and is central to arguments that
 340 lapse rate feedback is a contributor to AA. Based on radiosonde observations, Serreze et al. (1992) reported that
 341 temperature inversions (extremely strong stability), nearly ubiquitous over the ice-covered Arctic Ocean, tend to be
 342 surface-based from October through April, increasing in strength from October through winter in both depth and in
 343 the temperature difference from inversion base to top. For example, in October the median inversion depth is about
 344 900-m and the temperature difference is about 9K, whereas corresponding values in March are 1200 m and 12K. In
 345 summer, inversions are shallower and often elevated, with often a deep mixed layer below. (There are also
 346 commonly shallow melt-induced surface-based inversions.) The seasonal cycle over Arctic land areas is similar but
 347 with temperature differences across the inversion of 14-16K (Figure 6).

348 Figure 7 shows a vertical cross section of potential temperature from the equator to 90°N for October. Potential
 349 temperature increases with altitude more steeply in the Arctic than at other latitudes, illustrating its stronger static
 350 stability. The much stronger vertical stability of the Arctic troposphere compared to lower latitudes is obvious. In
 351 turn, a larger vertical extent of warming in October compared to December would be expected given that stability
 352 increases from autumn into winter. In terms of potential temperature, at 80°N (for example) the increase in potential
 353 temperature from the surface to 850 hPa in October is 10K, versus 15K in December. From the surface to 700hPa,
 354 potential temperature increases by 20K in October versus 25K in December. The atmosphere starts to cool freely to
 355 space at around 5-6 km above the surface (roughly the 500 hPa level). While pronounced autumn warming does not
 356 extend upwards that far (Figure 5), the results nevertheless argue that radiative cooling to space is more efficient in
 357 autumn than in winter, and that as amplified warming AA progresses, cooling to space will become more efficient as
 358 a negative feedback on autumn warming.



359

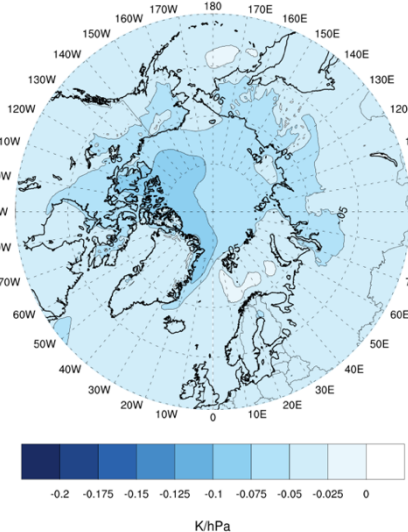
360 **Figure 6:** Monthly median inversion top (top of bars), base (bottom of bars) and temperature difference (solid lines) from
 361 (a) drifting station data from the central Arctic Ocean; (b) station Zhigansk over the Siberian tundra, taken as
 362 representative of the region [from Serreze et al., 1992, by permission of AMS].



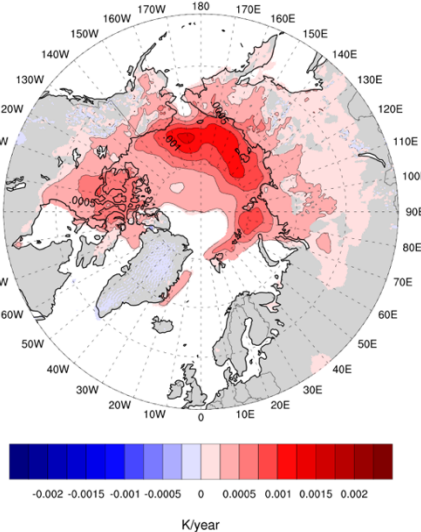
363

364 **Figure 7:** Vertical cross section of zonally averaged potential temperature (K) from the equator to the pole for October,
 365 averaged over the period 1981-2010.

(a) Oct Average dtheta/dp 1000-850 hPa 1980-2024



(b) Oct trend in dtheta/dp /year 1000-850 hPa 1980-2024



366

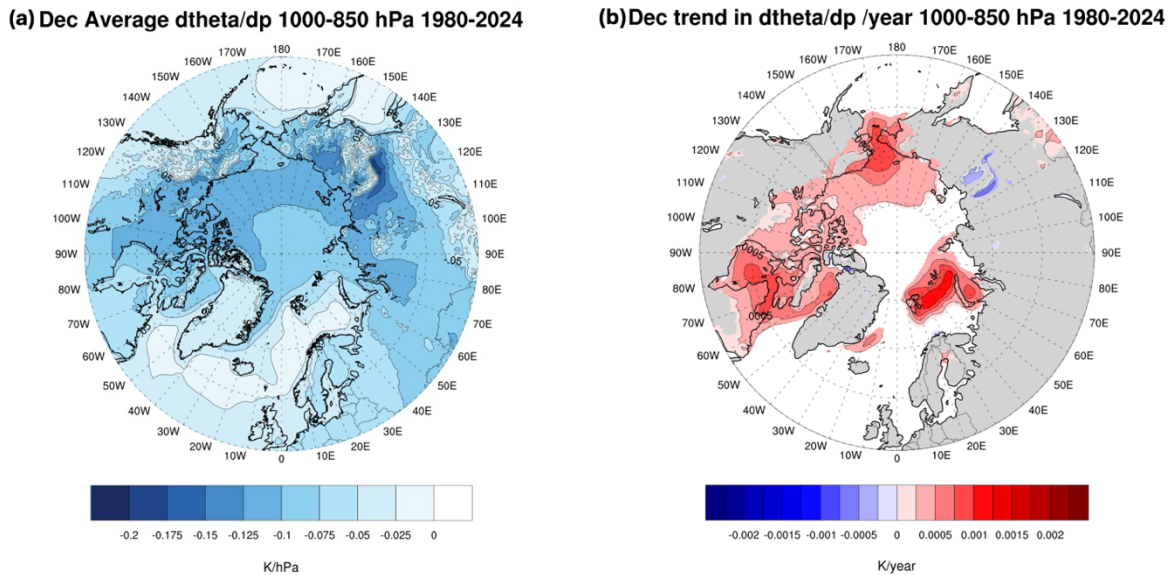
367 **Figure 8. Climatological averages ($\theta_{850} - \theta_{1000}$) / (850 hPa - 1000 hPa) and linear trends ($\theta_{850} - \theta_{1000}$) / (850 hPa - 1000 hPa per year) in low-level vertical stability**
 368 **expressed as ($\theta_{850} - \theta_{1000}$) / (850 hPa - 1000 hPa) Climatological averages and linear trends in low-level vertical stability**
 369 **(from surface to the 850 hPa level) expressed as change in potential temperature over 1000-850 hPa for October. Trends**
 370 **are in units of K/hPa per year.** Positive numbers in-for the climatological averages mean weaker stability, positive values
 371 **for trends mean a decrease in stability with time. Only trends significant at $p < 0.05$ are shaded- based on an ordinary least**
 372 **squares regression test. Shading is used for trends significant at $p < 0.05$.**

373 Figure 8 shows climatological averages of surface to 850 hPa static stability for October, along with linear trends. In
 374 a stable atmosphere, $d\theta/dP$ is negative (potential temperature increases with height while pressure decreases), so
 375 more negative values mean stronger stability. Consistent with Figure 7, there is a general increase in average stability
 376 moving polewards. However, stability is strongest north of Greenland and the Canadian Arctic Archipelago. It is likely
 377 not a coincidence that these areas have the thickest sea ice in the Arctic, implying especially small heat fluxes through
 378 the ice. Not surprisingly, large trends toward weaker static stability (positive values) dominate all the areas along the
 379 Eurasian coast, corresponding to the largest declineownward trends in September ice concentration, as well as in the
 380 Barents Sea, which has seen declinedownward trends in winter. Smaller trends towards weaker stability
 381 dominate most of the rest of the Arctic Ocean, likely driven by a thinning ice pack. While the average October
 382 conductive heat fluxes through most of the ice cover in October isare on the order of $5-10 \text{ W m}^{-2}$ (upward), Liu and
 383 Zhang (2025) found that the conductive heat fluxes hashave increased since 1979 due to thinning, which
 384 outcompetes the effect of positiveupward trends in surface skin temperatures. Our analysis finds support in the
 385 study of Simmonds and Li (2021) who find strong decreases in the Brunt-Vaisala frequency over the Arctic and its broader
 386 region. We note here that the B-V frequency contains a 1/theta term which highlights the impact in the colder regions.

387 Corresponding results for December follow in Figure 9. Average stability is generally stronger than for October, with
 388 the clear exception of the Norwegian and Barents Seas and the extreme northern North Atlantic, where there is near

389 neutral stability. The Norwegian and Barents Seas, in particular, ~~have been~~ are recognized for unstable near-surface
 390 boundary layers in winter that develop during cold air outbreaks as Arctic air moves over open water surfaces,
 391 promoting strong surface heat fluxes and convective-type precipitation (Olaffson and Oakland, 1994). Trends towards
 392 weaker stability are in turn prominent in the Barents Sea, the southern Chukchi Sea and Baffin and Hudson Bays, all
 393 areas where winter ice losses have been pronounced (especially the Barents Sea). Interesting in this regard is that
 394 weakening winter stratification may lead to intensification of near surface winds by increasing downward momentum
 395 transfer (Zappolini and Goessling, 2024), which will then foster stronger upward turbulent heat fluxes.

396 We stress that assessments of atmospheric stability and trends should be viewed with some caution. Based on
 397 comparisons with radiosonde profiles at coastal sites, Serreze et al. (2012) found that all three of the most modern
 398 reanalyses available at the time of that study (MERRA, NOAA CFSR, ERA-Interim) have positive cold-season
 399 temperature (and humidity) biases below the 850 hPa level and consequently ~~do~~ not capture observed low-level
 400 temperature and humidity and temperature inversions. MERRA ~~had~~ has the smallest biases. Graham et al. (2019)
 401 similarly found a positive winter 2-m temperature bias in all six atmospheric reanalyses they compared to sea ice
drifting stations – including ERA5. While they offer that the reanalyses are either not assimilating the radiosonde data
at low levels or are giving these data a low weight, problems in assimilating satellite data are likely involved. Further
analysis is warranted to assess whether ERA5 suffers from the same shortcomings. Additionally~~Indeed~~
 402 Wang and Zhao (2024) found that the depiction of static stability over the Arctic in summer appears to be sensitive to the
 403 reanalysis product examined (ERA5, NCEP-R2 and JRA-55).



407
 408 **Figure 9. Climatological averages (K_a, K/hPa) and linear trends (K_b, K/hPa per year) in low-level vertical stability**
 409 **(expressed as (0₈₅₀ - 0₁₀₀₀) / (850 hPa - 1000 hPa)) expressed as change in potential temperature over 1000-850 hPa for**
 410 **December. Trends are in units of K/hPa per year. Positive numbers in for the climatological averages mean weaker stability,**
 411 **positive values for trends mean a decrease in stability with time. Only trends significant at p<0.05 are shaded based on an**
 412 **ordinary least squares regression test. Shading is used for trends significant at p<0.05.**

413 **4 Discussion and Conclusions**

414 The results presented here show a clear association between patterns of autumn and winter sea ice concentration trends
415 and both the year-to-year evolution and seasonal expression of Arctic temperature anomalies. The link with sea ice
416 loss can be viewed as an expression of seasonally delayed albedo feedback. We also see signals of variable
417 atmospheric circulation in both temperature trends and the spatial structure of LAAs by decade. As discussed, a suite
418 of other processes can also be linked to Arctic Amplification. Given that any process leading to warming will tend to
419 enhance sea ice melt (spring and summer) or discourage its formation (autumn and winter), ~~it they~~ can be viewed as
420 serving to reinforce the key role of sea ice loss on observed AA.

421 Consider in this regard studies from coupled models showing that AA can arise without the albedo feedback through
422 the lapse rate and Planck feedbacks (e.g., Caballero and Langen, 2005; Pithan and Mauritsen, 2014; Previdi et al.,
423 2021). Lapse rate feedback relates to the stronger stability of the Arctic atmosphere compared to low latitudes,
424 focusing the temperature rise closer to the surface and reducing longwave radiative cooling to space. From coupled
425 simulations, Previdi et al. (2021) find that through positive lapse rate feedback, AA develops in only a few months
426 following an instantaneous quadrupling of atmospheric CO₂, well before any significant sea ice loss, although ice loss
427 contributes significantly to warming after the first few months. While one can question what an instantaneous
428 quadrupling of CO₂ teaches us about the real world, a key point is once sea ice begins to decline, the positive lapse
429 rate feedback, keeping the heating near the surface, will contribute to spring and summer ice melt and delay seasonal
430 ice growth. That static stability becomes stronger from autumn into winter indicates that focusing the heating near the
431 surface will also be more effective in winter. Conversely, ice loss, and likely also heat fluxes, are changing the larger
432 environment towards reduced stability at low levels.

433 Turning to the Planck feedback, the larger increase in Arctic temperatures required to bring the system back to
434 radiative equilibrium in response to a forcing can also be seen as a process augmenting summer sea ice loss and
435 delaying autumn and winter ice growth. Increased autumn cloud cover as a contributor to AA is closely tied to sea ice
436 loss through reducing stability in the boundary layer, promoting large upward surface heat fluxes (e.g., Kay and
437 Gettleman, 2012).

438 In parting, a key message stemming from the present study is that the process of AA must consider both its strong
439 seasonality and that AA, which is generally assessed by comparing Arctic regional temperature trends against trends
440 for the globe as a whole, comes about by the integration across the Arctic of large spatial heterogeneity of temperature
441 changes, seen both in the spatial pattern of Arctic trends but especially when we look at the problem through local
442 amplification anomalies – LAAs. While AA is small in summer, ~~evolving~~ summer processes, namely, ~~leading to~~ the
443 reduction of sea ice concentration and enhanced energy gain in the mixed layer, set the stage for the strong regional
444 expressions of AA in autumn. ~~These changes and the change~~ in spatial patterns of temperature anomalies ~~extend~~ into
445 winter as areas of open water freeze over. In all seasons, variable atmospheric circulations appear to be important.
446 ~~those in s~~Anomalous ~~summer~~ circulation ~~can~~ affect~~ting~~ spatial patterns of September ice extent. ~~and those in~~ In autumn
447 and winter, these anomalous circulation patterns can ~~affect~~ting temperature through advection as well as by their

448 influence on sea ice concentration, such as in the Barents Sea. Static stability also changes seasonally, which will
449 influence the vertical expression of temperature anomalies.

450 -In short, the more we look at AA, the more we discover that it is a very complex beast. These complexities bear not
451 only on the future evolution of AA and related impacts on permafrost warming and changes in the frequency of rain
452 on snow events (Serreze et al., 2021), but on key issues such as potential impacts of Arctic warming on middle latitude
453 weather patterns (Ding et al., 2024).

454 *Code and data availability:* The ERA5 data were obtained from the Research Data Archive at the National Center for
455 Atmospheric Research: DOI: 10.5065/BH6N-5N20. Sea ice data was obtained from the National Snow and Ice Data
456 Center <https://nsidc.org/data/nsidc-0051/versions/2>. For processing code contact Elizabeth Cassano
457 (Elizabeth.Cassano@colorado.edu)

458 *Author contributions:* Mark Serreze wrote the first draft of the paper. -Elizabeth Cassano performed the bulk of the
459 data analysis and creation of figures and assisted in writing. -Alex Crawford, John Cassano and Chen Zhang provided
460 intellectual input to the paper and contributed to the writing.

461 *Competing interests.* The contact author has declared that none of the authors has any competing interests.

462 *Acknowledgement:* This study was supported by NSF Navigating the New Arctic Grant 1928230 and the Canada-150
463 Chair Program.

464

465 **References**

466 AMAP, Arctic Climate Change Update 2021: Key trends and impacts. Summary for policy-makers, Arctic Monitoring
467 and Assessment Programme (AMAP), Oslo, Norway, 2021.

468 Arrhenius, 1896: On the influence of carbonic acid in the air upon the temperature of the ground. Philos. Mag. J. Sci.,
469 5, 237-276.

470 Barrett, A.P., Stroeve, J.C., and Serreze, M.C.: Arctic Ocean Precipitation from atmospheric reanalyses and
471 comparisons with North Pole drifting station records, Journal of Geophysical Research: Oceans, 125(1).
472 <https://doi.org/10.1029/2019jc015415>, 2020.

473 Beer, E., Eisenman, I., and Wagner, T. J.: Polar amplification due to enhanced heat flux across the halocline, Geophys.
474 Res. Lett., 47, <https://doi.org/10.1029/2019GL086706>, 2020.

475 Bianco, E., Lovino, D., Masina, S., Materia, S., and Ruggieri, P.: The role of upper-ocean heat content in the regional
476 variability of Arctic sea ice at sub-seasonal timescales, The Cryosphere, 18, 2357–2379, <https://doi.org/10.5194/tc-18-2357-2024>, 2024.

478 Bradley, R.S., Kemig, F.T. and Diaz, H.F.: Climatology of surface-based inversions in the North American Arctic, J.
479 Geophys. Res. Atmospheres, 97(D14), 15699- 15712, <https://doi.org/10.1029/92JD01451>, 1992.

480 Caballero, R., and Langen, P.: The dynamic range of poleward energy transport in an atmospheric general circulation
481 model, Geophys. Res. Lett., 32, L02705, doi:10.1029/2004GL021581, 2005.

482 Crawford, A. D., Lukovich, J. V., McCrystall, M. R., Stroeve, J. C., and Barber, D. G.: Reduced sea ice enhances
 483 intensification of winter storms over the Arctic Ocean, *J. Climate*, 35(11), 3353–3370. <https://doi.org/10.1175/jcli-d-21-0747.1>, 2022.

485 Crawford, A., Soriot, C., and Stroeve, J.: Autumn pauses in Arctic-wide sea-ice expansion, *J. Glaciol.*, 71, e21,
 486 <https://doi.org/10.1017/jog.2024.106>, 2025.

487 Dai, A., Luo, D., Song, M., and Liu, J.: Arctic amplification is caused by sea-ice loss under increasing CO₂, *Nat. Comm.*, 10, 121, <https://doi.org/10.1038/s41467-018-07954-9>, 2019.

489 Ding, S.S., Chen, X., Zhang, X., Zhang, X., and Xu, P.: A review on the Arctic-midlatitudes connection: Interactive
 490 impacts, physical mechanisms and nonstationary, *Atmosphere*, 15, 20.33980/atmoss15091115, 2024.

491 [Esau, I., Pettersson, L. H., Cancet, M., Chapron, B., Chernokulsky, A., Donlon, C., Johannessen, J. A.: The arctic](#)
 492 [amplification and its impact: A synthesis through satellite observations. *Remote Sensing*, 15\(5\), 1354, 2023..](#)

493 Fetterer, F., Knowles, K., Meier, W., and Savoie, M.: Sea Ice Index, digital media, National Snow and Ice Data Center,
 494 Boulder, Colorado, 2002.

495 [Gong, T., Feldstein, S., and Lee, S. : The role of downward infrared radiation in the recent Arctic winter warming](#)
 496 [trend. *J. Climate*, 30, 4937–4949, https://doi.org/10.1175/JCLI-D-16-0180.1, 2017.](#)

497 Graham, R. M., Cohen, L., Ritzhaupt, N., Segger, B., Graversen, R. G., Rinke, A., et al.: Evaluation of six atmospheric
 498 reanalyses over Arctic sea ice from winter to early summer, *J. Climate*, 32(14), 4121–4143,
 499 <https://doi.org/10.1175/jcli-d-18-0643.1>, 2019.

500 Graversen, R. G., and Burtu, M. Arctic amplification enhanced by latent energy transport of atmospheric planetary
 501 waves, *Quart. J. Roy. Meteor. Soc.*, 142, 2046–2054, 2016.

502 [Henderson, G. R., Barrett, B. S., Wachowicz, L. J., Mattingly, K. S., Preece, J. R., and Mote, T. L.: Local and](#)
 503 [remote atmospheric circulation drivers of Arctic change: A review. *Frontiers in Earth Science*, 9, 709896, 2021.](#)

504 Hersbach and Coauthors: The ERA5 global reanalysis, *Quart. J. Roy. Meteor. Soc.*, 146, 1999–2049,
 505 <https://doi.org/10.1002/qj.3803>, 2020.

506 Hurrell, J.W.: Decadal trends in the North Atlantic Oscillation: Regional temperatures and precipitation, *Science*–,
 507 269, 676-679, 1995.

508 Hurrell, J.W.: Influence of variations in extratropical wintertime teleconnections on Northern Hemisphere
 509 temperature, *Geophys. Res. Lett.*, 23, 665-668, 1996.

510 Jansen, E., Christensen, J.H., Dokken, T., Nisancioglu, K.H., Vintgher, B.M., Capron, E., Guo, C., Jensem, M.F.,
 511 Langen, P.L., Pedersen, R.A., Yang, S., Bentsen, M., Kjaer, H.A., Sadatzki, H., Sessford, E., and Stendel, M.: Past
 512 perspectives on the present era of abrupt Arctic climate change, *Nat. Clim. Change*, 10, 714–721, 2020.

513 Kahl, J.D., Serreze, M.C., and Schnell, R.C.: Tropospheric low-level temperature inversions in the Canadian Arctic,
 514 *Atmosphere-Ocean*, 30, 522-529, <https://www.tandfonline.com/doi/abs/10.1080/07055900.1992.9649453>, 1992

515 Kapsch, M.-L., Graversen, R.G., and Tjernström, M.: Springtime atmospheric energy transport and the control of
 516 Arctic summer sea-ice extent, *Nat. Climate Change*, 3, 744–748, doi:10.1038/nclimate1884, 2013.

517 Kay, J. E., and Gettelman, A.: Cloud influence on and response to seasonal Arctic sea ice loss, *J. Geophys. Res.*, 114,
 518 D18204, doi:10.1029/2009JD011773, 2009

519 Krishnan, S. et al.: The roles of the atmosphere and ocean in driving Arctic warming due to European aerosol
 520 reductions, *Geophys. Res. Lett.*, 47, e2019GL086681, 2020.

521 [Landy, J. C., Dawson, G. J., Tsamados, M., Bushuk, M., Stroeve, J. C., Howell, S. E. L., Krumpen, T., Babb, D. G.,](#)
 522 [Komarov, A. S., Heorton, H. D. B. S., Belter, H. J., and Aksenov, Y.: A year-round satellite sea-ice thickness record](#)
 523 [from CryoSat-2. *Nature*, 609, 517–522, https://doi.org/10.1038/s41586-022-05058-5, 2022.](#)

524 Lebrun, M., M. Vancoppenolle, Madec, G., and Massonnet, F.: Arctic sea-ice-free season projected to extend into
 525 autumn. *The Cryosphere*, 13, 79–96, <https://doi.org/10.5194/tc-13-79-2019>, 2019.

526 [Li, M., Lui, D., Simmonds, A., Dai A., Zhong, L. and Yao, Y., 2021: Anchoring of atmospheric teleconnection](#)
 527 [patterns by Arctic Sea ice loss and its link to winter cold anomalies in East Asia, *Int. J. Climatol.*, **41**, 547–558,](#)
 528 [2021.](#)

529

530 [Lee, S., Gong, T., Feldstein, S. B., Screen, J. A., and Simmonds, I. \(2017\): Revisiting the cause of the 1989–2009](#)
 531 [Arctic surface warming using the surface energy budget: Downward infrared radiation dominates the surface fluxes.](#)
 532 [Geophysical Research Letters, **44**\(20\), 10-654, 2017.](#)

533

534 [Li, M., Lui, D., Simmonds, A., Dai A., Zhong, L. and Yao, Y., 2021: Anchoring of atmospheric teleconnection](#)
 535 [patterns by Arctic Sea ice loss and its link to winter cold anomalies in East Asia, *Int. J. Climatol.*, **41**, 547–558,](#)
 536 [2021.](#)

537 Li, Z., Ding, Q., Steele, M., and Schweiger, A.: Recent upper Arctic Ocean warming expedited by summertime
 538 atmospheric processes, *Nat. Commun.*, **13**, 362, <https://doi.org/10.1038/s41467-022-28047-8>, 2022.

539 Lien, V. S., Schlichtholz, P., Skagseth, Ø., and Vikebø, F. B.: Wind-driven Atlantic water flow as a direct mode for
 540 reduced Barents Sea ice cover, *Journal of Climate*, **30**, 803–812, <https://doi.org/10.1175/jcli-d-16-0025.1>, 2017.

541 Liu, Y., and Zhang, J.: [Conductive heat flux over Arctic sea ice from 1979 to 2022. *J. Geophys. Res.* **130**: e2024JC022062 doi: 10.1029/2024JC022062, 2025. Conductive heat flux over Arctic sea ice from 1979 to 2022, *J. Geophys. Res. Oceans*, \[Luo, B., Luo, D., Dai, A., Simmonds, I., and Wu, L.: Decadal variability of winter warm Arctic-cold Eurasia dipole\]\(https://doi.org/10.1029/2024JC022062, 2025.</p>
<p>544 <a href=\)
 545 \[patterns modulated by Pacific Decadal Oscillation and Atlantic Multidecadal Oscillation. *Earth's Future*, **10**,\]\(#\)
 546 \[e2021EF002351, doi: 10.1029/2021EF002351, 2022.\]\(#\)](#)

547 Markus, T., J. C. Stroeve, J.C., and Miller, J.: [2009: Recent changes in Arctic sea ice melt onset, freezeup, and melt](#)
 548 [season length. *Journal of Geophysical Research*, **114**, C12024, <https://doi.org/10.1029/2009jc005436>, 2009.](#)

549 Mudryk, L.R., Chereque, A.E., Derksen, C., Loujus K. and Decharme, B.: Terrestrial Snow Cover, NOAA Arctic
 550 Report Card 2023, doi: 10.25923/xqwa-h543, 2023.

551 Navarro, J.A., Varma, V., Riipinen, I., Selander, O., Kirkevag, A., Struthers, H., Iversen, T., Hansson, H.-C., and Ekman,
 552 A.M.L.: Amplification of Arctic warming by past air pollution reductions in Europe, *Nature Geosci.*, **9**, 277–281,
 553 <https://doi.org/10.1038/ngeo2673>, 2016.

554 Olaffson, H., and Okland, E.: Precipitation from convective boundary layers in Arctic air masses, *Tellus A*, **46**(4–13), <https://doi.org/10.3402/tellusa.v46i1.15422>, 1994.

556 Park, H.-S., Lee, S., Kosaka, Y., Son, S.-W., and Kim, S.-W.: The impact of Arctic winter infrared radiation on early
 557 summer sea ice, *J. Climate*, **28**, 6281–6296, doi:10.1175/JCLI-D-14-00773.1, 2015.

558 Parkinson, C.L., Cavalieri, D.J., Gloersen, P., Zwally, H.J., and Comiso, J.C.C., Arctic sea ice extent, areas and
 559 trends, 1989–1996, *J. Geophys. Res.*, **104**, 20,837–20,856, 1999.

560 [Perovich, D. K. and Polashenski, C.: Albedo evolution of seasonal Arctic sea ice, *Geophys. Res. Lett.*, **39**, 8, \[Perovich, D. K. and Polashenski, C.: Albedo evolution of seasonal Arctic sea ice, *Geophys. Res. Lett.*, **39**, 8, \\[https://doi.org/10.1038/ngeo2071\\]\\(https://doi.org/10.1029/2012GL051432, 2012.</p>
<p>567 Pithan, F., and Mauritsen, T.: Arctic amplification dominated by temperature feedbacks in contemporary climate

 568 models, <i>Nature Geosci.</i>, 7, 181–184, <a href=\\), 2014.\]\(https://doi.org/10.1029/2012GL051432, 2012.</p>
<p>562 Perovich, D.K., Light, B., Eicken, H., Jones, K.F., Runciman, K. and Nghiem, S.V.: Increasing solar heating of the

 563 Arctic Ocean and adjacent seas, 1979–2005: Attribution and the role of ice-albedo feedback, <i>Geophys. Res. Lett.</i>, 34,

 564 L19505, doi: 10.1029/2007GL031480, 2007.</p>
<p>565 <a href=\)](#)

569 Previdi, M., K.L. Smith, K.L., and L.M. Polvani, L.M.: Arctic amplification of climate change: a review of underlying
 570 mechanisms. *Env. Res. Lett.*, **16**, 093003, doi:10.1088/1748-9326/ac1c29, 2021.

571 Rantanen M., Karpechko A.Y., Lipponen, A., Nordling, K., Hyvärinen, O., Ruosteenoja, K., Vihma T., and
 572 Laaksonen, A.: The Arctic has warmed nearly four times faster than the globe since 1979, *Nature Communications*
 573 *Earth and Environment*, **3**, 168, <https://doi.org/10.1038/s43247-022-00498-3>, 2022.

574 Renfrew, I. A., Barrell, C., Elvidge, A. D., Brooke, J. K., Duscha, C., King, J. C., et al.: An evaluation of surface
575 meteorology and fluxes over the Iceland and Greenland Seas in ERA5 reanalysis: The impact of sea ice distribution,
576 *Quart. J. Roy. Meteor. Soc.*, 147(734), 691–712, <https://doi.org/10.1002/qj.3941>, 2021.

577 Richter-Menge, J., and Druckenmiller, M. L. (eds.) The Arctic [In “State of the Climate in 2019”], *Bull. Am. Meteor.*
578 *Soc.*, 101, S239–S285, (2020).

579 [Rohde, R.A., and Hausfather, Z.: The Berkeley Earth Land/Ocean Temperature Record. Earth Sys. Sci. Data., 12, 3469-3479, https://doi.org/10.5194/essd-12-3469-2020, 2020.](#)

580

581 [Scott, M. \(2022\): “Why use the 1981 to 2010 average for sea ice?” National Snow and Ice Data Center. Accessed 11](#)
582 [Sep 2025. https://nsidc.org/learn/ask-scientist/why-use-1981-2010-average-sea-ice, 2022.](#)

583 [Sereen, J., and Simmonds, I.: The central role of diminishing sea ice in recent Arctic temperature amplification, Nature, 464, 1334–1337, https://doi.org/10.1038/nature09051, 2010a.](#)

584

585 Screen, J.A., and Simmonds, I.: The central role of diminishing sea ice in recent Arctic temperature amplification, *Nature*, 464, 1334–1337, doi:10.1038/nature09051, 2010a.

586

587 [Screen, J., and I. Simmonds: Increasing fall–winter energy loss from the Arctic Ocean and its role in Arctic](#)
588 [temperature amplification. Geophys. Res. Lett., 37, L16707, doi:10.1029/2010GL044136, 2010b.](#)

589 [Serreze, M.C., Kahl, J.D. and Schnell, R.C.: Low level temperature inversions of the Eurasian Arctic and comparisons](#)
590 [with Soviet drifting station data, J. Climate, 5, 615–629, https://doi.org/10.1175/1520-](#)
591 [0442\(1992\)005<0615:LLTIOT>2.0.CO;2, 1992. https://journals.ametsoc.org/view/journals/clim/5/6/1520-](#)
592 [0442_1992_005_0615_lltot_2_0_co_2.pdf, 1992.](#)

593 [Serreze, M.C., Walsh, J.E., Chapin, F.S., III, Osterkamp, T., Dyurgerov, M., Romanovsky, V., Oechel, W.C., Morison,](#)
594 [J., Zhang, T., and Barry, R.G.: Observational evidence of recent change in the northern high latitude environment,](#)
595 [Climatic Change, 46, 159–207, 2000.](#)

596 [Serreze, M., Barrett, A., Stroeve, J., Kindig, D., and Holland, M.: The emergence of surface-based Arctic](#)
597 [amplification. Cryosphere, 3, https://doi.org/10.5194/tc-3-11-2009, 2009.](#)

598 Serreze, M.C., Barrett, A.P., and Stroeve, J.: Recent changes in tropospheric water vapor over the Arctic as assessed
599 from radiosondes and atmospheric reanalyses. *Journal of Geophysical Research*, 117, D10104, doi:
600 10.1029/2011JD017421, 2012.

601 Serreze, M.C., Gustavson, J., Barrett, A.P., Druckenmiller, M.L., Fox, S., Voveris, J., Stroeve, J., Sheffield, B., Forbes,
602 B.C., Rasmus, S., Laptander, R., Brook, M., Brubaker, M., Temte, J., McCrystal, M., and Bartsch, A.: Arctic rain on
603 snow events: bridging observations to understand environmental and livelihood impacts. *Environmental Research*
604 *Letters*, 16, <https://doi.org/10.1088/1748-9326/ac269b>, 2021

605 [Serreze, M.C., Kahl, J.D. and Schnell, R.C.: Low level temperature inversions of the Eurasian Arctic and comparisons](#)
606 [with Soviet drifting station data, J. Climate, 5, 615–629, https://doi.org/10.1175/1520-](#)
607 [0442\(1992\)005<0615:LLTIOT>2.0.CO;2, 1992. https://journals.ametsoe.org/view/journals/clim/5/6/1520-](#)
608 [0442_1992_005_0615_lltot_2_0_co_2.pdf, 1992.](#)

609 [Serreze, M.C., Walsh, J.E., Chapin, F.S., III, Osterkamp, T., Dyurgerov, M., Romanovsky, V., Oechel, W.C., Morison,](#)
610 [J., Zhang, T., and Barry, R.G.: Observational evidence of recent change in the northern high latitude environment,](#)
611 [Climatic Change, 46, 159–207, 2000.](#)

612 [Serreze, M., Barrett, A., Stroeve, J., Kindig, D., and Holland, M.: The emergence of surface-based Arctic](#)
613 [amplification. Cryosphere, 3, https://doi.org/10.5194/tc-3-11-2009, 2009.](#)

614 Siew, P.Y.F., Wu, Y., Ting, M., Zheng, C., Ding, O. and Seager, R.: Significant contribution of internal variability to
615 recent Barents–Kara sea ice loss in winter, *Comm. Earth Environ.*, 5, 411, <https://doi.org/10.1038/s43247-024-01582-6>, 2024.

617 [Simmonds, I. And Li, M.: Trends and variability in polar sea ice, global atmospheric circulations, and baroclinicity](#)
618 [Ann. NY Acad. Sci. 1504 167-86, 2021.](#)

619 [Smith, D.M., J.A. Screen, C. Deser, J. Cohen, J.C. Fyfe, J. García-Serrano, T. Jung, V. Kattsov, D. Matei, R. Msadek,](#)
620 [Y. Peings, M. Simmonds, J. Ukita, J.-H. Yoon, and X. Zhan: The Polar Amplification Model Intercomparison Project](#)

621 [https://doi.org/10.5194/gmd-12-1139-2019, 2019.](https://doi.org/10.5194/gmd-12-1139-2019)

622

623 Stammerjohn, S., Massom, R. Rind, D., and Martinson, D.: Regions of rapid sea ice change: An inter-hemispheric
624 seasonal comparison, *Geophys. Res. Lett.*, 39, L06501, doi: 10.1029/2012GL080874, 2012.

625 Steele, M., Ermold, W., and Zhang, J.: Arctic Ocean surface warming trends over the past 100 years, *Geophys. Res.*
626 *Lett.*, 35, L02614, doi:10.1029/2007GL031651, 2008.

627 [Stroeve, J. and Notz, D.: Changing state of Arctic sea ice across all seasons. *Env. Res. Lett.*, 13, 10300,](https://doi.org/10.1088/1748-9326/aade56)
628 [Stroeve, J.C., Markus,T., Boisvert, L., Miller, J., and Barrett, A.: Changes in Arctic melt season and implications for](https://doi.org/10.1088/1748-9326/aade56, 2018.</p><p>629 <a href=)
630 [2016: Using timing of ice retreat to predict timing of fall freeze-](https://doi.org/10.1002/2013GL058951, 2014.</p><p>631 Stroeve, J. C., A. D. Crawford, and S. Stammerjohn, <a href=)
632 [up in the Arctic. *Geophysical Research Letters*, 43, 6332–6340,](https://doi.org/10.1002/2016gl069314)
633 [https://doi.org/10.1002/2016gl069314, 2016.](https://doi.org/10.1002/2016gl069314)

634 [Stroeve, J.C., Markus,T., Boisvert, L., Miller, J., and Barrett, A.: Changes in Arctic melt season and implications for](https://doi.org/10.1002/2013GL058951)
635 [Stroeve, J. and Notz, D.: Changing state of Arctic sea ice across all seasons, *Env. Res. Lett.*, 13, 10300,](https://doi.org/10.1002/2013GL058951, 2014.</p><p>636 <a href=)
637 [Sumata, H., Steur, L. de, Divine, D. V., Granskog, M. A., and Gerland, S.: Regime shift in Arctic Ocean sea ice](https://doi.org/10.1088/1748-9326/aade56, 2018.</p><p>638 Stuecker, M. F., Bitz, C.M., Armour, K.C, Proitosescu, Kang, S.M., Shang-Ping, Xie, Doyeon, K., McGregor., S.,
639 Zhang, W., Zhao, S., Cai, W., Dong, Y. and Jin, F-F.: Polar amplification dominated by local forcing and feedbacks,
640 <i>Nat. Clim. Change</i>, 8, 1076–1081, 2018.</p><p>641 <a href=)
642 [Taylor, P. C., Boeke, R. C., Boisvert, L. N., Feldl, N., Henry, M., Huang, Y., and Tan, I.: Process drivers, inter-](https://doi.org/10.1038/s41586-022-05686-x, 2023.</p><p>643 <a href=)
644 [model spread, and the path forward: A review of amplified Arctic warming. *Frontiers in Earth Science*, 9, 758361,](https://doi.org/10.31233/osf.io/75836)
645 [Tian, T., Yang, S., Hoyer, J. L., Nielsen-Englyst, P., and Singha, S.: Cooler Arctic surface temperatures simulated](https://doi.org/10.31233/osf.io/75836, 2022.</p><p>646 Thompson, D.W.J, and Wallace, J.M.: The Arctic Oscillation signature in the wintertime geopotential height and
647 temperature fields, <i>Geophys. Res. Lett.</i> 25, 1297-1300, 1998.</p><p>648 <a href=)
649 [by climate models are closer to satellite-based data than the ERA5 reanalysis. *Communications Earth &*](https://doi.org/10.1038/s41560-023-11111-1)

650 [Environment, 5\(1\), 111, 2024.](https://doi.org/10.1038/s41560-023-11111-1)

651 Timmermans, M.-L., Toole, J., and Krishfield, R.: Warming of the interior Arctic Ocean linked to sea ice losses at the
652 basin margins, *Sci. Adv.*, 4, eaat6773, [https://doi.org/10.1126/sciadv.aat6773, 2018.](https://doi.org/10.1126/sciadv.aat6773)

653 Walsh, J. E.: Intensified warming of the Arctic: Causes and impacts on middle latitudes, *Glob. Planet. Change* 117,
654 52–63, 2014.

655 [Wang, C., Graham, R. M., Wang, K., Gerland, S., and Granskog, M. A.: Comparison of ERA5 and ERA-Interim](https://doi.org/10.1029/2018EA000576)
656 [near surface air temperature, snowfall and precipitation over Arctic sea ice: effects on sea ice thermodynamics and](https://doi.org/10.1029/2018EA000576)
657 [evolution. *The Cryosphere*, 13\(6\), 1661–1679, 2019.](https://doi.org/10.1029/2018EA000576)

658 Wang, X. and Zhao, J.: Trends and oscillations in arctic mediterranean atmospheric static stability during recent Arctic
659 warming. *Climate and Atmospheric Science*, [https://www.nature.com/articles/s41612-024-00576-7, 2024.](https://www.nature.com/articles/s41612-024-00576-7)

660 Wang, Y., F. Huang, and T. F.: Spatio-temporal variations of Arctic amplification and their linkage with the Arctic
661 oscillation. *Acta Oceanol. Sin.*, 36, 42–51, [https://doi.org/10.1007/s13131-017-1025-z, 2017.](https://doi.org/10.1007/s13131-017-1025-z)

662 [Wang, C., Graham, R. M., Wang, K., Gerland, S., and Granskog, M. A.: Comparison of ERA5 and ERA-Interim](https://doi.org/10.1029/2018EA000576)
663 [near-surface air temperature, snowfall and precipitation over Arctic sea ice: effects on sea ice thermodynamics and](https://doi.org/10.1029/2018EA000576)
664 [evolution. *The Cryosphere*, 13\(6\), 1661–1679, 2019](https://doi.org/10.1029/2018EA000576)

665 Wexler, H.: Cooling in the lower atmosphere and the structure of polar continental air, *Mon. Wea. Rev.*, 64, 122-
666 136, 1936.

667 Woods, C. and Caballero, R.: The role of moist intrusions in winter Arctic warming and sea ice decline, *J. Clim.*, 29,
668 4473–4485, <https://doi.org/10.1175/JCLI-D-15-0773.1>, 2016.

669 Wu, D.L., and Lee, J.N.: Arctic low cloud changes as observed by MISR and CALIOP: Implication for the enhanced
670 autumnal warming and sea ice loss, *J. Geophys. Res.*, 117, D07107, doi: 10.1029/2011JD017040, 2012.

671 Yu, L., Zhong, S., Vihma, T., and Sun, B.: Attribution of late summer early autumn Arctic sea ice decline in recent
672 decades, *npj Clim. Atmos. Sci.* 4, 3, 2021a.

673 Yu, Y., Xiao, W., Zhang, Z., Cheng, X., Hui, F., and Zhao, J.: Evaluation of 2-m air temperature and surface
674 temperature from ERA5 and ERA-I using buoy observations in the Arctic during 2010–2020. *Remote Sensing*,
675 13(14), 2813, 2021b.

676 Zappolini, M., and Goessling, H.F.: Atmospheric destabilization leads to Arctic Ocean winter surface wind
677 intensification, *Nature Communications Earth and Environment*, <https://doi.org/10.1038/s43247-024-01428-1>,
678 2024.

679 Zhang, C., Cassano, J. J., Seefeldt, M. W., Wang, H., Ma, W., and Tung, W.: Quantifying the impacts of atmospheric
680 rivers on the surface energy budget of the Arctic based on reanalysis. *The Cryosphere*, 19, 4671–4699,
681 <https://doi.org/10.5194/tc-19-4671-2025>, 2025.

682 Zhou, W., Yao, Y., Luo, D., Simmonds, I., and Huang, F.: The key atmospheric drivers linking regional Arctic
683 amplification with East Asian cold extremes. *Atmos. Res.* 283, 106557, doi: 10.1016/j.atmosres.2022.106557, 2023

684 Zhou, W., Leung, L. R., and Lu, J.: Steady threefold Arctic amplification of externally forced warming masked by
685 natural variability. *Nat. Geosci.*, 17, 508–515, <https://doi.org/10.1038/s41561-024-01441-1>, 2024.